Biochemistry and Biophysics Reports 8 (2016) 107–113

Contents lists available at ScienceDirect

Biochemistry and Biophysics Reports

journal homepage: www.elsevier.com/locate/bbrep

High-throughput flow cytometry screening of human hepatocellular carcinoma reveals CD146 to be a novel marker of tumor-initiating cells

Kui Chen [a], Avrilynn Ding [a], Yu Ding [a], Anand Ghanekar [a,b,*]

[a] Toronto General Research Institute, University Health Network, 101 College St., Toronto, Ontario, Canada M5G 1L7
[b] Division of General Surgery, University Health Network, 585 University Avenue, Toronto, Ontario, Canada M5G 2N2

ARTICLE INFO

Article history:
Received 4 April 2016
Received in revised form
2 August 2016
Accepted 9 August 2016
Available online 12 August 2016

Keywords:
Cancer
Hepatocellular carcinoma
Tumor-initiating cell
Stem cell
Flow cytometry
CD146

ABSTRACT

Hepatocellular carcinoma (HCC) remains a common and lethal cancer. Cancer stem cells, or tumor-initiating cells (TICs), are thought to contribute to the pathogenesis of HCC, but remain to be fully characterized. Unbiased screens of primary human HCC cells for the identification of novel HCC TIC markers have not been reported. We conducted high-throughput flow cytometry (HT-FC) profiling to characterize the expression of 375 CD antigens on tumor cells from 10 different human HCC samples. We selected 91 of these for further analysis based on HT-FC data that showed consistent expression in discrete, rare, sortable populations of HCC cells. Nine of these CD antigens demonstrated significantly increased expression in the $EpCAM^+$ stem/progenitor fraction of a human HCC cell line and were further evaluated in primary human HCC tissues from 30 different patients. Of the nine tested, only CD146 demonstrated significantly increased expression in HCC tumor tissue as compared with matched adjacent non-tumor liver tissue. $CD146^+CD31^-CD45^-$ cells purified from HCC tumors and cell lines demonstrated a unique phenotype distinct from mesenchymal stem cells. As compared with other tumor cell fractions, $CD146^+CD31^-CD45^-$ cells showed significantly increased colony-forming capacity *in vitro,* consistent with TICs. This study demonstrates that HT-FC screening can be successfully applied to primary human HCC and reveals CD146 to be a novel TIC marker in this disease.

1. Introduction

Hepatocellular carcinoma (HCC)[1] is the 5th most common cancer worldwide and the 3rd most common cause of cancer death [1]. Although curative surgery is possible for patients with early-stage HCC, patients with advanced disease have a median survival of less than one year [2]. The development of more effective clinical strategies requires an improved understanding of HCC pathobiology.

The cell of origin from which HCC arises remains controversial. The cancer stem cell model suggests that tumors are hierarchically organized and sustained by a distinct population of tumor-initiating cells (TICs) that self-renew while generating the full repertoire of tumorigenic and non-tumorigenic cells in a tumor [3]. Several lines of evidence support the existence of TICs in human HCC. Clinically defined subgroups of HCC are associated with transcriptional profiles that mimic embryonic liver and liver progenitor cells [4,5]. Targeted analyses of human HCC cell lines and patient samples for cell populations expressing a variety of surface markers previously shown to identify TICs in other solid tumors have revealed analogous populations in HCC that are capable of anchorage-independent growth and colony formation *in vitro* as well as tumor initiation *in vivo* in immunodeficient mice [6–14]. However, *unbiased* screens of primary human HCC cells conducted for the purpose of identifying novel HCC TIC populations have not been reported. Novel HCC TIC markers are needed because the cellular populations identified by the existing repertoire of HCC TIC markers are relevant in only a small fraction of clinical HCC samples, failing to account for the biology of tumorigenesis in the full spectrum of clinical HCC samples that demonstrate significant genetic diversity and heterogeneity [15]. Identification of novel TIC markers may reveal novel mechanisms of tumorigenesis in HCC and expose targets for innovative new therapeutic strategies.

In this report, we describe the use of a high-throughput flow cytometry (HT-FC) screening platform [16] to interrogate the expression of a large number of cluster of differentiation (CD)

* Correspondence to: 11 PMB 171, Toronto General Hospital, University Health Network, 585 University Avenue, Toronto, ON, Canada M5G 2N2.
E-mail address: anand.ghanekar@uhn.ca (A. Ghanekar).

[1] CD – cluster of differentiation; DMEM - Dulbecco's Modified Eagle Medium; FACS – fluorescence activated cell sorting; FBS – fetal bovine serum; HCC – hepatocellular carcinoma; HMSC-he – human liver-derived mesenchymal stem cells; HT-FC – high throughput flow cytometry; IMDM – Iscove's Modified Dulbecco's Medium; MCAM – melanoma cell adhesion molecule; MEF – mouse embryonic fibroblast; MSC – mesenchymal stem cell; MSCM – mesenchymal stem cell medium; TIC – tumor initiating cell.

http://dx.doi.org/10.1016/j.bbrep.2016.08.012

antigens on patient-derived human HCC cells in an unbiased fashion in order to identify candidate molecules for further characterization as novel TIC markers. We further demonstrate how application of this strategy in combination with secondary screening methods reveals CD146 to be a novel TIC marker in human HCC.

2. Materials and methods

2.1. Cell cultures

Human HCC cell lines PLC/PRF/5 (ATCC) and Huh7 (gift from Dr. Paolo Parini, Karolinska Institute, Sweden) were cultured in Dulbecco's Modified Eagle Medium (DMEM) (Gibco) containing 4500 mg/L D-glucose, 10% fetal bovine serum (FBS) and 1 × MEM non-essential amino acids (Gibco). Human liver-derived mesenchymal stem cells (HMSC-he) and mesenchymal stem cell medium (MSCM) were purchased from ScienCell Research Laboratories (Carlsbad, CA, USA) and maintained according to the manufacturer's instructions. Primary human HCC tissue collection and tumor cell isolation were conducted as previously described [17], under an institutionally approved protocol and with patient consent. Irradiated mouse embryonic fibroblast (MEF) feeder cells (gift from Dr. Gordon Keller, University Health Network, Toronto, Canada) were maintained in Iscove's Modified Dulbecco's Medium (IMDM) (Gibco) containing 10% FBS. Culture medium was changed every 3 days.

2.2. Antibodies and reagents

374 fluorochrome-conjugated antibodies against cell surface CD antigens (except CD133) in four 96-well HT-FC plates, prepared as previously described [16], were obtained from the laboratory of Dr. Laurie Ailles, University Health Network, Toronto, Canada. Anti-human CD133/1-APC (AC133) antibody (Miltenyi Biotec) was added separately. Anti-human EpCAM-PE (9C4), CD19-PE (5E10), CD31-APC (WM59), CD44-APC (BJ18), CD45-PE-Cy7 (HI30), CD90-PE (5E10), CD105-APC (43A3), CD146-AF488 (SHM-57), CD166-PE (3A6), Stro-1-AF647 antibodies and PE/Cy5 Streptavidin were purchased from BioLegend. CD31-Biotin (9G11) was obtained from R&D Systems Inc. LIVE/DEAD® Fixable Violet Dead Cell Stain Kit (405 nm excitation) and SYTOX® Blue Dead Cell Stain dye were obtained from Life Technologies. CompBead Plus Anti-Mouse Ig, κ beads were obtained from BD Biosciences. Human FcR Blocking Reagent (Miltenyi Biotec) was used to block nonspecific binding.

2.3. Flow cytometry

Immunostaining and flow cytometry analyses were performed according to standard procedures. Cultured PLC/PRF/5, Huh7 or HMSC-he cells were dissociated into single cell suspensions by using StemPro® Accutase® Cell Dissociation Reagent (Life Technologies). Subsequent analysis or sorting were conducted on BD LSR II flow cytometer or BD FACS Aria II cell sorter (Becton-Dickinson). Fluorescence-minus-one controls were generated for each antibody used and compensations were set using BD Plus CompBeads and FACS Diva software.

2.4. High throughput flow cytometry (HT-FC)

Immunostaining was performed as previously described [16] with some modifications. 40 million primary HCC cells were blocked in human FcR Blocking Reagent, incubated with CD45 PE-Cy7 antibody, then diluted in 20 ml staining buffer and aliquoted into four HT-FC plates (50 ul, 0.1 million cells per well). After HT-FC staining, cells were incubated with LIVE/DEAD® Fixable Violet dye followed by 4% paraformaldehyde fixation, then resuspended with 1XPBS (250 μL /well) for further analysis. Data collection was performed on a BD LSR II flow cytometer with an attached high throughput sampler. Plates were read under the standard throughput mode with loader settings as follows: 3.0 μL/sec sample flow rate, 200 μL sample volume, 75 μL mixing volume, 200 μL/sec mixing speed, 4 mixes, 400 μL wash volume. 80,000 events were collected per well. The HT-FC workflow and flow cytometer gating strategy is illustrated in Supplementary Fig. S1. Target events were collected and analyzed within the $CD45^-$ cell population.

2.5. PLC/PRF/5 cell sorting and quantitative real-time PCR screening

$EpCAM^+$ and $EpCAM^-$ PLC/PRF/5 cell subsets were sorted separately into 96 well plates with 1 cell per well and cultured for 14 days. Colonies were amplified to 12 well and 6 well plates followed by T25 flasks, and EpCAM status confirmed by flow cytometry. Total RNA was prepared using PureLink RNA Mini Kit (Life Technologies) from PLC/PRF/5 $EpCAM^{+/-}$ colonies and 30 human HCC tumor/adjacent paired tissues. MVP™ Human Liver Total RNA pool (Agilent Technologies) was introduced as a normalization zero control. cDNA was synthesized using SuperScript® III Reverse Transcriptase (Life Technologies). Real-time PCR and relative quantitative analysis was carried out as previously described [18]. Primer sequences are provided in Supplementary Table S1.

2.6. Colony-forming assay

$CD146^+$ and $CD146^-$ Huh7 cells were sorted into 6 well plates at a density of 1000 cells per well and cultured for 14 days. Cells were fed with new culture medium every 3 days. Colonies were fixed with glutaraldehyde (6.0% w/v), stained with crystal violet (0.5% w/v) and counted using a stereomicroscope. Irradiated MEF feeder cells were seeded in 96 well plates at 90% confluency and cultured with IMDM/FBS medium for 24 h then maintained in KnockOut™ DMEM medium plus 20% KnockOut™ Serum Replacement. $CD146^-CD45^-CD31^-$, $CD146^+CD45^-CD31^+$ and $CD146^+CD45^-CD31^-$ HCC cells were sorted into 96 well MEF feeder cell plates with different density and limiting dilution analysis (LDA) was conducted after 21 days as previously described [19].

2.7. Data analysis

FCS 3.0 files were exported to FlowJo v9.3. In all cases, dead cells and doublets were excluded prior to analyzing marker expression. Gates were set using fluorescence-minus-one controls, and percent-positive values were exported to Excel file for use in further statistical analysis and generation of heat maps. p values were calculated using GraphPad Prism software. Heat maps were generated using MultiExperiment Viewer software [20].

3. Results

3.1. HT-FC profiling of human HCC samples

We performed HT-FC analysis of primary HCC cells isolated from the tumors of 10 different patients. Demographic and clinical information pertaining to these patients is shown in Supplementary Table S2. In this cohort of patients, the mean age was 59.1 ± 9.1 years, 7 of 10 were male, most suffered from chronic viral hepatitis, and all of the HCC tumors were moderately differentiated.

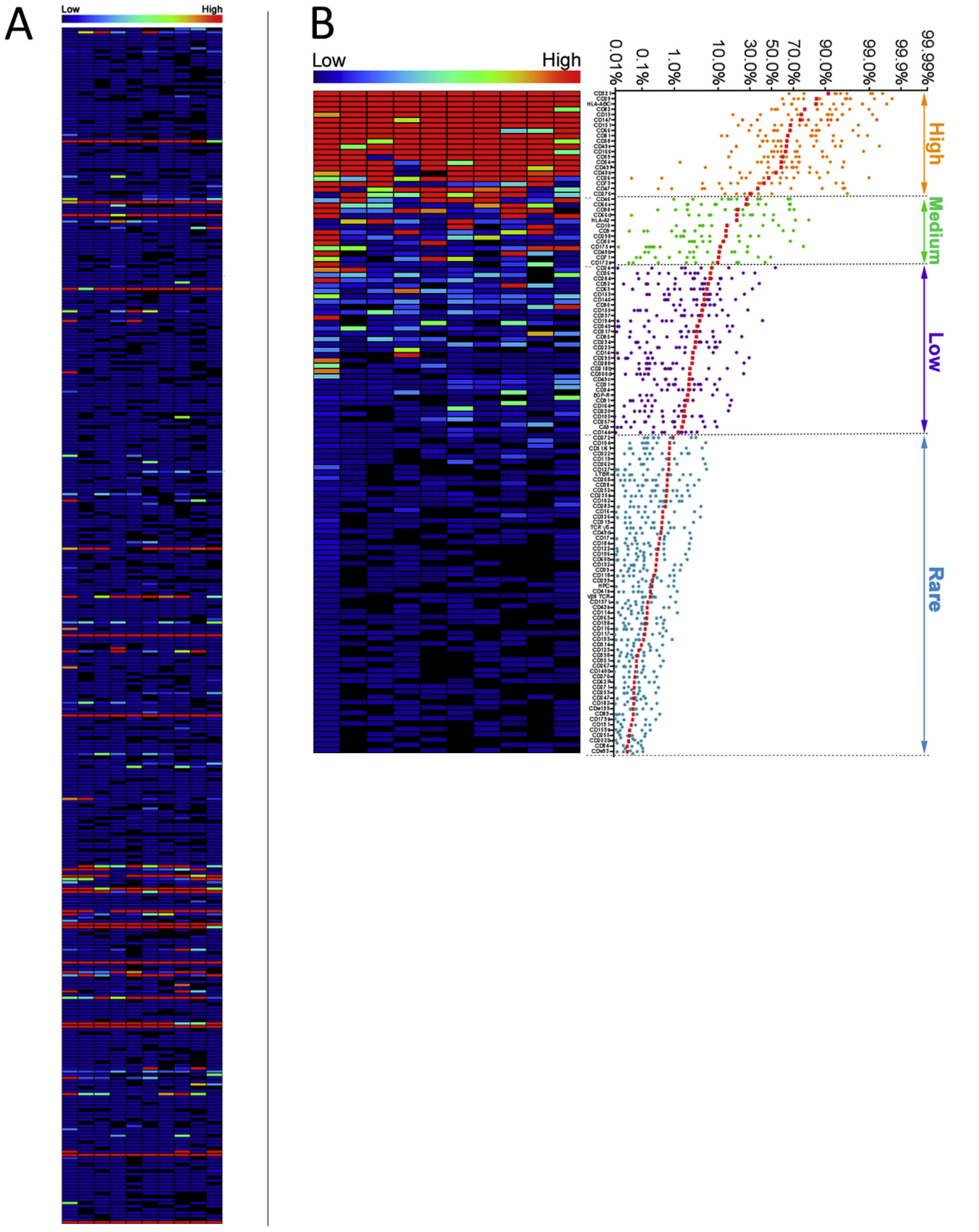

Fig. 1. HT-FC profiling was carried out to characterize the expression of 375 unique CD antigens on tumor cells from 10 unique human HCC samples. A) Heatmap generated from the complete dataset with each column corresponding to a different HCC sample and each row corresponding to a different CD antigen. B) Heatmap and dot-plot representation of 125 CD antigens expressed by a mean of at least 1% of HCC cells across the 10 samples, ordered from most commonly to least commonly expressed exactly as organized in Supplementary Table S3.

The fraction of cells expressing each CD antigen in each patient sample is illustrated in a heatmap in Fig. 1A, demonstrating similar patterns of CD antigen expression across the various patient samples. Interestingly, the proportion of HCC cells from primary patient tumor samples expressing HCC TICs identified in previous studies varied considerably. For example, CD13 was expressed on 76.10 ± 8.72% of cells, CD24 on 7.79 ± 5.33%, CD90 on 5.29 ± 0.84%, CD44 on 0.041 ± 0.019%, EpCAM on 0.50 ± 0.46%, and CD133 on 0.0051 ± 0.0034% [6–12]. As illustrated in Fig. 1B, we stratified 125 antigens with consistent expression in the majority of patients into groups based on the mean proportion of cells demonstrating antigen expression as follows: High - > 30%, Medium – 10–30%, Low – 1–10%, Rare - < 1%. The raw data for these 125 antigens is provided in Supplementary Table S3.

3.2. Secondary screening of HT-FC data

In order to identify novel candidate HCC TIC markers from the HT-FC data, we developed a secondary screening strategy working from the widely accepted principle that TICs are discrete, relatively rare populations of cells within tumors [3].

We first manually reviewed the HT-FC plots and identified 91 CD antigens from the low/rare expression groups that marked discrete, sortable populations of cells from the HCC samples.

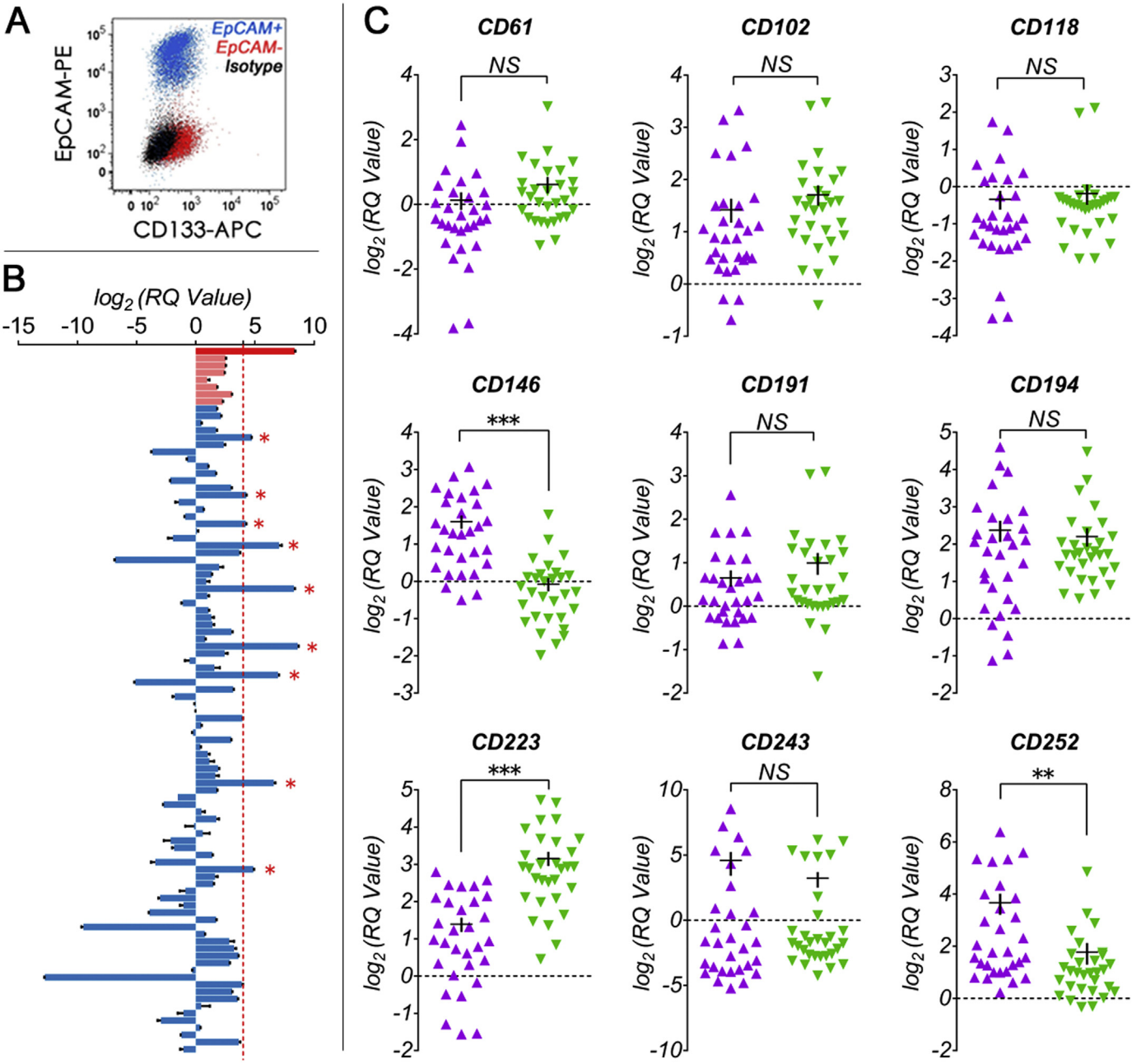

Fig. 2. A) Flow cytometry plot demonstrating discrete, sortable populations of EpCAM$^+$ stem/progenitor subpopulation (blue) and EpCAM$^-$ control cells (red) in the human HCC cell line PLC/PRF/5. B) Quantitative RT-PCR analysis demonstrating mRNA levels of EpCAM (top dark red bar), 7 stemness genes (CD133, Oct 3/4, Nanog, SOX2, Bmi1, Notch2, CTNNB1) (light red bars ordered from top down), and 91 candidate TIC markers (blue bars ordered from top down exactly as organized in Supplementary Table S1) in EpCAM$^+$ PLC/PRF/5 cells; red asterisks denote 9 genes with most highly increased expression; error bars represent ± SEM. C) Dot plots demonstrating quantitative RT-PCR analysis of mRNA levels of the 9 genes identified in panel B in 30 human HCC tumor tissues (purple) and matched adjacent non-tumor liver tissue (green) normalized against expression in MVP™ human liver control mRNA. Horizontal lines represent the mean, and error bars represent ± SEM. NS, non-significant,*** $p < 0.001$. (For interpretation of the references to color in this figure legend, the reader is referred to the web version of this article.)

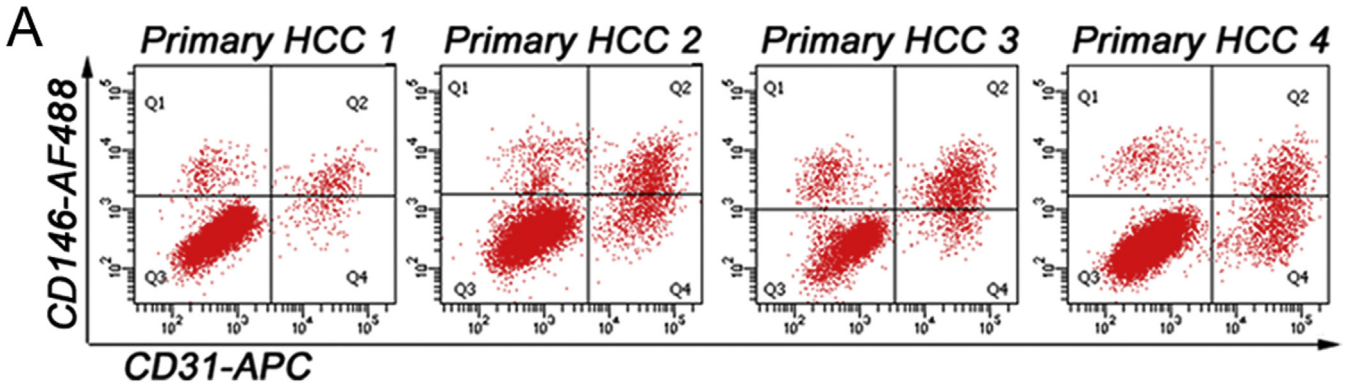

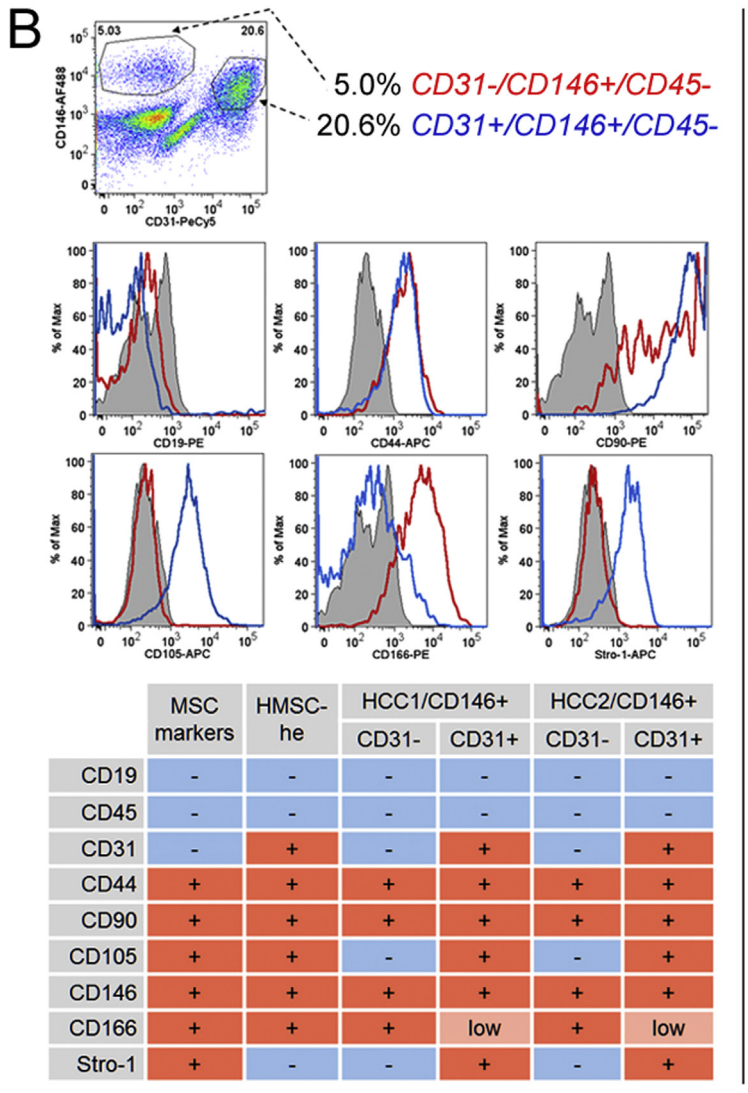

	MSC markers	HMSC-he	HCC1/CD146+		HCC2/CD146+	
			CD31-	CD31+	CD31-	CD31+
CD19	-	-	-	-	-	-
CD45	-	-	-	-	-	-
CD31	-	+	-	+	-	+
CD44	+	+	+	+	+	+
CD90	+	+	+	+	+	+
CD105	+	+	-	+	-	+
CD146	+	+	+	+	+	+
CD166	+	+	+	low	+	low
Stro-1	+	-	-	+	-	+

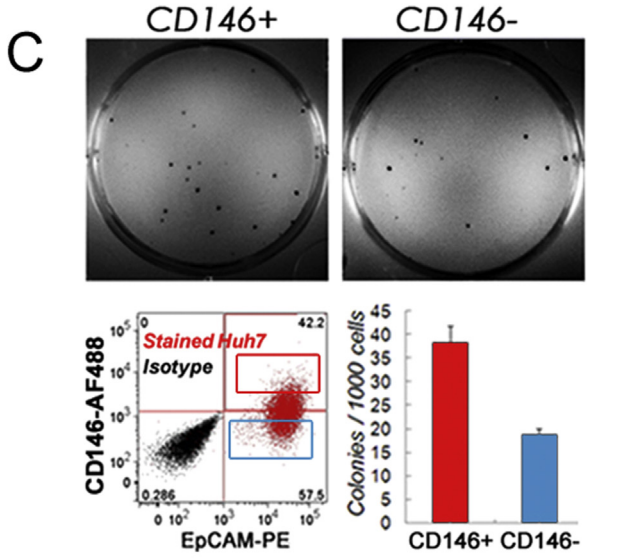

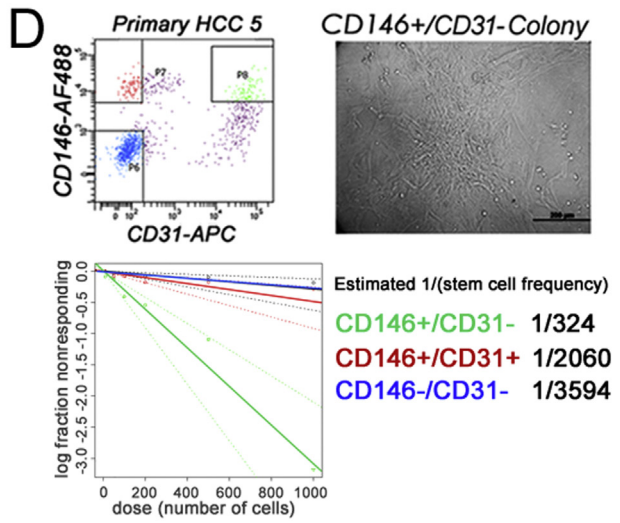

Fig. 3. A) Flow cytometry plots demonstrating CD146 and CD31 expression in tumor cells isolated from four unique primary human HCC samples. All events were analyzed in the CD45$^-$ fraction. B) Representative flow cytometry plots and expression summary table of CD146$^+$CD31$^-$CD45$^-$ human HCC cells (red) from two tumor samples (HCC1 and HCC2) demonstrating that this population lacks expression of CD105 and Stro-1 and thus has a phenotype distinct from the consensus MSC marker profile, CD146$^+$CD31$^+$CD45$^-$ HCC cells (blue), and HMSC-he cells (staining shown in Supplementary Fig. S2). Isotype controls are depicted in grey. C) Photographic image of 6-well plates demonstrating that CD146$^+$ cells isolated by flow cytometry from the human HCC cell line Huh7 demonstrate a greater colony-forming capacity than the CD146$^-$ fraction, quantified in the bar graph. D) Representative plot demonstrating three subpopulations (CD146$^+$CD31$^-$, CD146$^+$CD31$^+$, CD146$^-$CD31$^-$) purified by flow cytometry from the CD45$^-$ fraction of primary human HCC tumor samples and cultured at limiting dilution on MEFs to assess colony-forming capacity (phase contrast microscope image of representative colony shown). Using the principles of serial limiting dilution analysis [19], varying numbers of cells from each population were separately plated and the number of colonies that were generated in each sample well were subsequently counted. The number of input cells per well that did not generate a colony (*i.e.* total number of input cells – total number of colonies generated) was then plotted against the total number of input cells to reveal an estimate for the TIC frequency as a proportion of the input cell number for each purified cellular population, using the widely utilized principles of limiting dilution analysis [19]. Estimated values of 1/stem cell frequency for the three subpopulations reveal that CD146$^+$CD31$^-$ cells are the most highly enriched for TICs. The TIC frequency within the CD146$^+$CD31$^-$ population was estimated to be 1/324, six times more common than in the CD146$^+$CD31$^+$ population and 11 times more common than in the CD146$^-$ CD31$^-$ population. (For interpretation of the references to color in this figure legend,the reader is referred to the web version of this article.)

To determine which of these CD antigens might reflect TICs, we analyzed their expression in the $EpCAM^+$ fraction of HCC cells, which are known to demonstrate tumor-initiating capacity and stem/progenitor cell features [10]. Discrete populations of $EpCAM^+$ and $EpCAM^-$ PLC/PRF/5 cells (Fig. 2A) were purified by fluorescence activated cell sorting (FACS). As shown in Fig. 2B, the $EpCAM^+$ fraction demonstrated an increased expression of stemness genes (CD133, Oct3/4, Nanog, SOX2, Bmi1, Notch2 and CTNNB1) as compared with the $EpCAM^-$ fraction, supporting their TIC phenotype. Fig. 2B also demonstrates the expression of the 91 candidate CD antigens in $EpCAM^+$ cells as compared with $EpCAM^-$ cells. As compared with $EpCAM^-$ cells, $EpCAM^+$ cells demonstrated greater than 16-fold increased expression of the following 9 CD antigens: CD61, CD102, CD118, CD146, CD191, CD194, CD223, CD243, and CD252.

To validate the predicted relevance of these antigens, we studied their expression in 30 primary human HCC samples as compared with matched adjacent non-tumor liver tissue. As shown in Fig. 2C, the expression of seven of these antigens was similar in tumor and non-tumor liver tissue. Only CD146 expression was significantly higher in HCC tissue as compared with non-tumor liver tissue, while CD223 expression was significantly lower.

3.3. Characterization of $CD146^+$ HCC cells

We utilized flow cytometry to analyze the expression of CD146 in HCC cells. As CD146 is known to be expressed on cells of the endothelial lineage [21,22], we incorporated the endothelial cell marker CD31 as well as the leukocyte marker CD45 into our staining protocols and gating/analysis strategies. As shown in Fig. 3A, $CD146^+CD31^-$ cells consisted of discrete, sortable populations in the $CD45^-$ fraction of tumor cells isolated from four unique fresh human HCC specimens. As CD146 is also recognized to be a marker of mesenchymal stem cells (MSCs)[23], we utilized flow cytometry to determine the expression of MSC markers on $CD146^+$ HCC cells from human tumor tissue. As shown in Fig. 3B, $CD146^+CD31^-CD45^-$ cells isolated from fresh human HCC samples have a unique phenotype distinct from MSCs, lacking expression of CD105 and Stro-1 (control staining of MSCs is shown in Supplementary Fig. S2).

To investigate the functional properties of $CD146^+CD31^-CD45^-$ HCC cells, we evaluated colony-forming capacity *in vitro* to measure the capability of single HCC cells to give rise to discrete colonies of HCC cells, as a surrogate for tumor-initiating capacity. As shown in Fig. 3C, $CD146^+$ cells from the human HCC cell line Huh7 demonstrated a higher colony-forming capacity than $CD146^-$ cells. Finally, we assayed the colony-forming capacity of $CD146^+CD31^-$ cells purified from the $CD45^-$ fraction of primary human HCC samples, as compared with $CD146^-CD31^-$and $CD146^+CD31^+$ cells. Using the principle of serial limiting dilution analysis [19], varying numbers of cells from each population were separately plated and the number of colonies that were generated in each sample well were subsequently counted. The number of input cells per well that did not generate a colony (*i.e.* total number of input cells – total number of colonies generated) was then plotted against the total number of input cells to reveal an estimate for the TIC frequency as a proportion of the input cell number for each purified cellular population, using the widely utilized method of limiting dilution analysis [19]. As shown in Fig. 3D, a significantly greater proportion of $CD146^+CD31^-$ formed colonies as compared with the other populations studied. The tumor-initiating cell frequency within the $CD146^+CD31^-$ population was estimated to be 1/324, six times more common than in the $CD146^+CD31^+$ population and 11 times more common than in the $CD146^-CD31^-$ population.

4. Discussion

In this report, we have demonstrated that HT-FC profiling can be successfully applied to primary human HCC cells. By utilizing a secondary screening step to filter the large initial expression dataset against an HCC cell line with a well defined stem/progenitor cell phenotype, we were able to generate a relatively short list of nine CD antigens that could be further studied as potential TIC markers in primary human HCC samples. This strategy has revealed CD146 to be a novel TIC marker in human HCC, with $CD146^+CD31^-CD45^-$ HCC cells demonstrating significant enrichment in colony-forming capacity *in vitro* as compared with other populations of HCC cells.

While prior reports of TIC markers in HCC have largely focused on evaluating the relevance of TIC markers identified in other cancers on HCC cell lines, the novel aspects of this study are that (i) the screening strategy was unbiased, and (ii) the analysis was focused on primary human HCC tissues obtained from fresh resection specimens. Furthermore, this is the first report demonstrating that CD146 identifies a unique population of cells in primary human HCC samples with functional tumor-initiating capacity, distinct from endothelial cells and MSCs. Although the $CD146^+CD31^-$ population identified in our study continues to express some markers seen on MSCs, we believe that the absence of Stro-1 and CD105 (expression of which constitutes “minimal defining criteria” for MSCs [24]) demonstrates that we have isolated a unique population of cells with a distinct phenotype that deserves further characterization. Interestingly, other markers seen on MSC have also been characterized as HCC TIC markers in prior studies, including CD90 and CD44 [8,25]. Although CD105 is known to be expressed on cells of the endothelial lineage, it is expressed on MSCs in the absence of CD31; thus, the absence of CD105 from the $CD31^-$ population further supports our hypothesis that the $CD146^+/CD31^-$ population of interest in our study is distinct from MSCs.

CD146, also known as melanoma cell adhesion molecule (MCAM) or cell surface glycoprotein MUC18, is a 113 kDa cell adhesion molecule which has been reported to be a marker for endothelial lineage cells (EPCs)[21] or for mesenchymal stem cells (MSCs) isolated from multiple adult and fetal organs . Recently, a variety of studies have suggested that CD146 plays a role in many cancers, including breast cancer [26,27], sarcoma [28], lung cancer [29], pancreatic cancer [30], cervical and endometrial cancer [31], esophageal cancer [32] and malignant melanoma [33]. Two recent studies found that CD146 expression was upregulated in HCC tissues and cell lines, was an adverse clinical prognostic factor, and promoted a variety of oncogenic cellular functions such as migration, invasion, and transcriptional/translational activation [34,35]. However, neither one of these studies specifically isolated or investigated the functional properties of $CD146^+$ cell populations purified from human HCC tissues. Interestingly, a recent study describing HT-FC screening of primary human sarcoma also identified CD146 as a novel TIC marker in this cancer [28], underscoring the relevance of our observations in HCC.

While we have demonstrated the *in vitro* colony-forming capacity of $CD146^+CD31^-CD45^-$ HCC cells as a surrogate for tumor-initiating capacity, we have not yet been able to directly assay *in vivo* tumor formation by these cells in immunodeficient mice due to the very small number of cells that can be isolated from primary HCC samples, which are of sufficient quantity to perform *in vitro* assays alone. Secondly, while we have demonstrated that the TIC frequency in the $CD146^+CD31^-CD45^-$ population is 1/324, we hope to find additional cell surface markers or other cellular properties within this population of cells that allow for the purification of subpopulations of cells that demonstrate even further enrichment of tumor-initiating capacity as compared with other tumor cells.

In conclusion, we have shown that the application of HT-FC for the unbiased cell surface marker profiling of primary human HCC tissues reveals CD146 as a novel TIC marker in this disease. In combination with the relevance of CD146 to cancer pathobiology demonstrated by other studies, our report provides further rationale for additional work to explore CD146 as a novel target for innovative therapeutics. By increasing the number of patient samples analyzed in this way and by combining with other secondary screening strategies, HT-FC is a viable novel platform for the discovery of important pathobiological aspects of human HCC.

Acknowledgments

This work was supported by an Operating Grant from the Cancer Research Society (Grant No. 19177).

Appendix A. Transparency document

Transparency document associated with this article can be found in the online version at http://dx.doi.org/10.1016/j.bbrep.2016.08.012.

References

[1] H.B. El-Serag, K.L. Rudolph, Hepatocellular carcinoma: epidemiology and molecular carcinogenesis, Gastroenterology 132 (2007) 2557–2576.
[2] J.M. Llovet, S. Ricci, V. Mazzaferro, et al., Sorafenib in advanced hepatocellular carcinoma, N. Engl. J. Med. 359 (2008) 378–390.
[3] J.E. Visvader, Cells of origin in cancer, Nature 469 (2011) 314–322.
[4] K.J. Yong, C. Gao, J.S. Lim, et al., Oncofetal gene SALL4 in aggressive hepatocellular carcinoma, N. Engl. J. Med. 368 (2013) 2266–2276.
[5] J.S. Lee, J. Heo, L. Libbrecht, et al., A novel prognostic subtype of human hepatocellular carcinoma derived from hepatic progenitor cells, Nat. Med. 12 (2006) 410–416.
[6] N. Haraguchi, H. Ishii, K. Mimori, et al., CD13 is a therapeutic target in human liver cancer stem cells, J. Clin. Investig. 120 (2010) 3326–3339.
[7] T.K. Lee, A. Castilho, V.C. Cheung, et al., CD24(+) liver tumor-initiating cells drive self-renewal and tumor initiation through STAT3-mediated NANOG regulation, Cell Stem Cell 9 (2011) 50–63.
[8] Z.F. Yang, D.W. Ho, M.N. Ng, et al., Significance of CD90+ cancer stem cells in human liver cancer, Cancer Cell 13 (2008) 153–166.
[9] R. Kim, S.B. Kim, E.H. Cho, et al., CD44 expression in patients with combined hepatocellular cholangiocarcinoma, Ann. Surg. Treat. Res. 89 (2015) 9–16.
[10] T. Yamashita, J. Ji, A. Budhu, et al., EpCAM^{-}positive hepatocellular carcinoma cells are tumor-initiating cells with stem/progenitor cell features, Gastroenterology 136 (2009) 1012–1024.
[11] S. Ma, K.W. Chan, L. Hu, et al., Identification and characterization of tumorigenic liver cancer stem/progenitor cells, Gastroenterology 132 (2007) 2542–2556.
[12] K.H. Tang, S. Ma, T.K. Lee, et al., CD133(+) liver tumor-initiating cells promote tumor angiogenesis, growth, and self-renewal through neurotensin/interleukin-8/CXCL1 signaling, Hepatology 55 (2011) 807–820.
[13] C.P. Zhu, A.Q. Wang, H.H. Zhang, et al., Research progress and prospects of markers for liver cancer stem cells, World J. Gastroenterol. 21 (2015) 12190–12196.
[14] T. Oikawa, Cancer stem cells and their cellular origins in primary liver and biliary tract cancers, Hepatology (2016).
[15] J. Zucman-Rossi, A. Villanueva, J.C. Nault, et al., Genetic landscape and biomarkers of hepatocellular carcinoma, Gastroenterology 149 (2015), 1226–1239 e4.
[16] C.A. Gedye, A. Hussain, J. Paterson, et al., Cell surface profiling using high-throughput flow cytometry: a platform for biomarker discovery and analysis of cellular heterogeneity, PLoS One 9 (2014) e105602.
[17] K. Chen, S. Ahmed, O. Adeyi, et al., Human solid tumor xenografts in immunodeficient mice are vulnerable to lymphomagenesis associated with Epstein-Barr virus, PLoS One 7 (2012) e39294.
[18] S.P. Cleary, W.R. Jeck, X. Zhao, et al., Identification of driver genes in hepatocellular carcinoma by exome sequencing, Hepatology 58 (2013) 1693–1702.
[19] Y. Hu, G.K. Smyth, ELDA: extreme limiting dilution analysis for comparing depleted and enriched populations in stem cell and other assays, J. Immunol. Methods 347 (2009) 70–78.
[20] A.I. Saeed, V. Sharov, J. White, et al., TM4: a free, open-source system for microarray data management and analysis, Biotechniques 34 (2003) 374–378.
[21] N. Bardin, V. Moal, F. Anfosso, et al., Soluble CD146, a novel endothelial marker, is increased in physiopathological settings linked to endothelial junctional alteration, Thromb. Haemost. 90 (2003) 915–920.
[22] S. Thomann, T. Longerich, A.V. Bazhin, et al., Selective targeting of liver cancer with the endothelial marker CD146, Oncotarget 5 (2014) 8614–8624.
[23] A. Sorrentino, M. Ferracin, G. Castelli, et al., Isolation and characterization of CD146+ multipotent mesenchymal stromal cells, Exp. Hematol. 36 (2008) 1035–1046.
[24] M. Dominici, K. Le Blanc, I. Mueller, et al., Minimal criteria for defining multipotent mesenchymal stromal cells. The International Society for Cellular Therapy position statement, Cytotherapy 8 (2006) 315–317.
[25] Z. Zhu, X. Hao, M. Yan, et al., Cancer stem/progenitor cells are highly enriched in CD133+CD44+ population in hepatocellular carcinoma, Int. J. Cancer 126 (2010) 2067–2078.
[26] G. Zabouo, A.M. Imbert, J. Jacquemier, et al., CD146 expression is associated with a poor prognosis in human breast tumors and with enhanced motility in breast cancer cell lines, Breast Cancer Res. 11 (2009) R1.
[27] Q. Zeng, W. Li, D. Lu, et al., CD146, an epithelial-mesenchymal transition inducer, is associated with triple-negative breast cancer, Proc. Natl. Acad. Sci. USA 109 (2012) 1127–1132.
[28] Q. Wei, Y.J. Tang, V. Voisin, et al., Identification of CD146 as a marker enriched for tumor-propagating capacity reveals targetable pathways in primary human sarcoma, Oncotarget 6 (2015) 40283–40294.
[29] S. Oka, H. Uramoto, Y. Chikaishi, et al., The expression of CD146 predicts a poor overall survival in patients with adenocarcinoma of the lung, Anticancer Res. 32 (2012) 861–864.
[30] B. Zheng, K. Ohuchida, Y. Chijiiwa, et al., CD146 attenuation in cancer-associated fibroblasts promotes pancreatic cancer progression, Mol. Carcinog. (2015).
[31] H. Zhang, J. Zhang, Z. Wang, et al., CD146 is a potential marker for the diagnosis of malignancy in cervical and endometrial cancer, Oncol. Lett. 5 (2013) 1189–1194.
[32] Y. Li, J.M. Yu, X.M. Zhan, et al., Correlation of CD146 expression and clinicopathological characteristics in esophageal squamous cell carcinoma, Oncol. Lett. 8 (2014) 859–863.
[33] D. Jean, J.E. Gershenwald, S. Huang, et al., Loss of AP-2 results in up-regulation of MCAM/MUC18 and an increase in tumor growth and metastasis of human melanoma cells, J. Biol. Chem. 273 (1998) 16501–16508.
[34] J. Wang, X. Tang, W. Weng, et al., The membrane protein melanoma cell adhesion molecule (MCAM) is a novel tumor marker that stimulates tumorigenesis in hepatocellular carcinoma, Oncogene 34 (2015) 5781–5795.
[35] G. Jiang, L. Zhang, Q. Zhu, et al., CD146 promotes metastasis and predicts poor prognosis of hepatocellular carcinoma, J. Exp. Clin. Cancer Res. 35 (2016) 38.